24th COBEM - 2017

24th ABCM International Congress of Mechanical Engineering
December 3-8, 2017, Curitiba, PR, Brazil

COBEM-2017-1223
MATHEMATICAL MODELING AND EXPERIMENTAL ANALYSIS FOR THE ELONGATED BUBBLE SHAPE IN TWO-PHASE SLUG FLOW

Mateus Weiland
Cristiane Cozin
Rômulo Rodrigues
Marco G. Conte
Fausto A. Barbuto
Rigoberto E.M. Morales
Multiphase Flow Research Center (NUEM), Federal University of Technology – Paraná (UTFPR), Curitiba, Brazil
mateusweiland@hotmail.com, criscozin@yahoo.com.br, romuloluisrodrigues@hotmail.com, mg_conte@hotmail.com, fausto_barbuto@yahoo.ca, rmorales@utfpr.edu.br

Abstract. *In gas-liquid two-phase flow, the phases distribute inside the pipe in different spatial configurations according to the flow characteristics, namely: the fluid flow rates, the properties of each phase and the geometric parameters of the pipeline. These different configurations are known as flow patterns. Slug flow is a pattern commonly found in oil and gas production lines. This flow pattern is defined by a unit cell comprising an aerated liquid slug and an elongated bubble surrounded by a liquid film. A possible approach to correctly characterize slug flow is the mathematical modeling around the elongated bubble shape. The numerical solution of this kind of modeling yields liquid and gas fractions, elongated bubble and liquid slug lengths. This study presents a literature review of theoretical models for the elongated bubble shape. Moreover, it analyzes experimental results for determining the influence of characteristic parameters of the two-phase slug flow on the elongated bubble shape.*

Keywords: *Slug flow, Elongated Bubble Shape, Two-Phase Flow Model, Liquid Film Model*

NOMENCLATURE

l_S	Liquid slug length
u_{LS}	Liquid slug velocity
u_{GS}	Dispersed bubbles velocity
l_B	Elongated bubble length
u_{LB}	Liquid film velocity
u_T	Elongated bubble velocity
u_{GB}	Gas velocity within the bubble zone
R_{LB}	Liquid holdup within the bubble zone.
R_{GB}	Void fraction within the bubble zone.
R_{LS}	Liquid holdup within the liquid slug zone
R_{GS}	Void fraction within the liquid slug zone
v_L	Liquid relative velocity
v_G	Gas relative velocity

ρ_L	Liquid specific mass
ρ_G	Gas specific mass
S_L	Liquid wet perimeter
S_G	Gas wet perimeter
S_I	Interfacial perimeter
τ_G	Shear stress between gas and wall
τ_L	Shear stress between liquid and wall
τ_I	Shear stress between gas and liquid
θ	Inclination of the tube
g	Gravity
A_L	Liquid transversal area
A_G	Gas transversal area
j_G	Gas superficial velocity
j_L	Liquid superficial velocity

1. INTRODUCTION

Multiphase flows in pipelines commonly show several patterns depending upon the industrial niche where those flows appear. In oil and gas production, for example, the slug flow pattern is very common, given the typical flow rates

occurring in this kind of operation. This pattern is characterized by the intermittent succession of an aerated liquid slug followed by an elongated bubble flowing atop a liquid film. These regions compose a unit cell (Wallis, 1969) and each present different characteristics along the pipe. The unit cell is showed in Fig. 1.

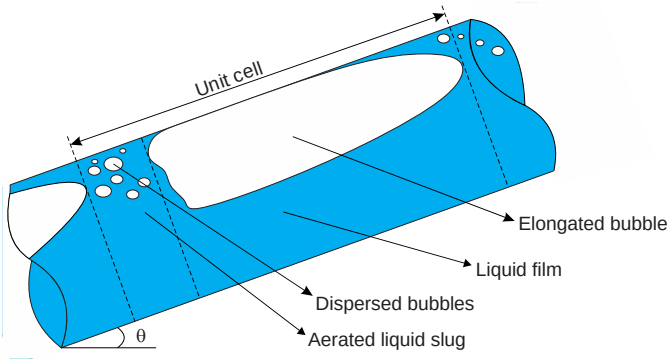

Figure 1. Unit cell

In literature, several authors worked on the elongated bubble shape. Dukler and Hubbard (1975) presented one of the first detailed bubble models. Such model is based on the observation that the liquid slug, by moving faster than the liquid film, captures part of the liquid in the said film, thus accelerating the scooped liquid up to the speed of the slug. The authors also validated their model using experimental data, by using an air-water system in a 3.81-cm horizontal glass tube with 19.8 m of length. Using electronic contact probes, those researchers measured the translation speed of the front of the bubble and, according to their claim, achieving good results. They also measured the length of the slug using a single electrical contact probe. A clock starts counting the time when the slug first contacts the probe until the contact is interrupted at the rear of the slug. Using this measured time and the velocity of the bubble they can determine the length of the slug. However, the authors warn that due to slug aeration it is difficult to use this technique for their measurement.

Bendiksen (1984) conducted an experimental study using air and water in a 1.92-cm acrylic tube. In this study, the author measures isolated bubbles in a flow. The author varies the slope of the pipe from -30° to + 90° (including horizontal flow) and uses a phototransistor to make the velocity measurements. The focus of his study is to find an equation to calculate the translational velocity of the unit cell. This velocity is of paramount importance to the model since it is used to calculate the length of the unit cell. Based on photographic evidence Bendiksen (1984) does not observe a stable bubble profile and reports that the most significant changes in the profile are the appearance of the hydraulic jump and bubbles dispersed in the tail of the bubble.

From the momentum equation for the liquid and for the gas in the region of the elongated bubble, Taitel and Barnea (1990) developed a model for horizontal, inclined and vertical slug flows. According to the authors' model, liquid and gas velocities in the slug flow may be different, with slippage occurring between dispersed bubbles and the liquid, unlike the Dukler and Hubbard (1975) model. The model requires four auxiliary relations: the unit cell translation velocity, liquid holdup in the liquid slug zone, the unit cell frequency and the velocity of bubbles dispersed in the liquid slug region. This model was the one chosen for implementation, since it considers all the inclinations from horizontal to vertical and can be numerically implemented in a simple way, obtaining results with low computational time.

Fagundes Netto et al (1999) present a theoretical and experimental study of the bubble shape. Water and gas were injected into a 0.053-m ID, 90-m long horizontal pipeline. The measurement section with 5 sensors (wire probes) was located 70 m from the inlet and, according to the authors, at this point developed bubbles with constant profile and traveling at a constant speed were found to exist. Similarly to Bendiksen (1984), the authors used isolated bubbles that reach a developed profile and travel at a constant speed a few meters from the beginning of the pipe. The authors also presented a more complex theoretical model where the bubble is divided into four regions, modeled separately: nose, body, hydraulic jump and tail. The input data for his model are the internal pipe diameter, liquid flow, velocity and bubble volume. However, the author validated his model for horizontal flows only. Still according to his conclusions, the profile of the bubble does not vary with its length.

The choice of the technique to be used to make a measurement of experimental data is a factor that greatly influences the results. Therefore, choosing the technique that best fits the problem is important. Falcone et al (2009) shows several techniques for measuring experimental data in multiphase flows. The authors explain the techniques and point out which one is the best for each situation, so that more accurate data can be obtained.

Rodrigues et al (2015) studied air-water flow in a 25.8-mm ID, 9.2-m long acrylic tubing. The slopes were 0º, -4º, -7º, -10º and -13º. The author measured void fractions in the cross-section using an electrode mesh sensor (wire mesh) and from the generated temporal signals he extracted statistical distributions for: the elongated bubble translation velocity, unit cell frequency, bubble length and liquid and void fractions in the elongate bubble region. In this work, 29

measurement points were used in a horizontal pipeline, but with different superficial velocities of liquid and gas. These points were used to validate the theoretical model proposed in the article.

Hanyang and Liejin (2016) also carried out an experimental and numerical study on the flow of a single elongated bubble in a horizontal and inclined intermittent flow. Their theoretical model is based on Fagundes Netto et al (1999) bubble model, but extends it for inclined flows. In their experiments, they used a 0.05-m ID, 16.5-m long pipe. Three pairs of conductive probes were used to measure the bubble shape. The authors obtained excellent results when the simulated and the experimentally measured bubble profiles were compared. According to the authors, the profile of the bubble depends on the Froude number, the bubble length and the pipe inclination.

The main purpose of this work is to investigate the experimental and simulated shapes of the elongated bubble in horizontal flows. A theoretical model based on the work of Taitel and Barnea (1990) is developed. The numerical solution of this model determines the liquid and gas fractions (R_{LB} , R_{GB}), elongated bubble and liquid slug lengths (l_B, l_S), and other variables of interest. The developed model can reasonably predict the bubble shapes in horizontal intermittent flows when compared with the experimental results.

2. MATHEMATICAL MODELING

2.1 Unit Cell

The unit cell shown in Figure 2 includes an aerated liquid slug and an elongated gas bubble surrounded by a liquid film. The length of the liquid slug l_S is measured as the space between the noses of two consecutive bubbles. u_{LS} is the average liquid velocity in the slug and u_{GS} is the average gas velocity in the dispersed bubbles. l_B is the length of the elongated bubble and u_{LB} is the average velocity of the liquid film. The front of the bubble moves with velocity u_T, which is not necessarily the same velocity as the average gas velocity u_{GB} inside the bubble. The liquid and gas fractions in the region of the elongate bubble are R_{LB} and R_{GB}, respectively. The liquid and gas fractions in the slug region are R_{LS} and R_{GS}, respectively.

2.2 Mathematical modeling

In order to obtain an equation capable of calculating the shape of the elongated bubble, the Taitel and Barnea (1990) work was used. The present work starts from the momentum equation for both the liquid and gas phases in the elongated bubble region, under the following hypotheses:

1- Steady state;
2- One-dimensional flow along the x-axis;
3- The liquid phase is incompressible;
4- Both phases are Newtonian;
5- Heat transfer and mass are neglected;
6- The bubbles are uniformly distributed in the slug;
7- There is only gas above the nose of the elongated bubble;
8- In a same cross section, the pressure gradient is the same for both phases;
9- The properties of both phases are constant in the cell unit;
10- The unit cell is moving at a constant velocity U_T .

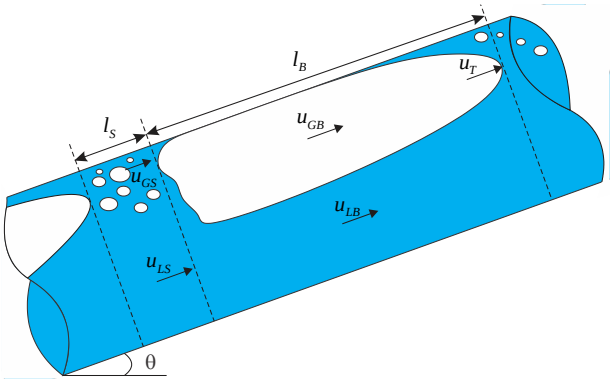

Figure 2. Cell Unit - Variables.

Eqs (1) and (2) are obtained when those hypotheses are applied to the momentum equations for the liquid and gas phases:

$$\rho_L v_L \frac{\partial v_L}{\partial x} = -\frac{\partial P}{\partial x}\cos\theta + \frac{\tau_L S_L}{A_L} - \frac{\tau_i S_i}{A_L} + \rho_L g \sin\theta - \rho_L g \cos\theta \frac{\partial h}{\partial x} \tag{1}$$

$$\rho_G v_G \frac{\partial v_G}{\partial x} = -\frac{\partial P}{\partial x}\cos\theta + \frac{\tau_G S_G}{A_L} - \frac{\tau_i S_i}{A_L} + \rho_L g \sin\theta - \rho_L g \cos\theta \frac{\partial h}{\partial x} \tag{2}$$

In the equations above, the first term represents the inertial term of the phase. The first term on the RHS represents the pressure gradient, the second term represents the phase friction with the pipe wall, the third term represents the friction in the gas-liquid interface, the fourth term represents the weight and the fifth term represents the hydrostatic pressure of the phase. Considering hypothesis #8 and isolating $\partial h/\partial x$ we obtain:

$$\frac{\partial h}{\partial x} = \frac{\overbrace{\frac{\tau_L S_L}{A_L} - \frac{\tau_G S_G}{A_G} - \tau_i S_i \left(\frac{1}{A_L} + \frac{1}{A_G}\right)}^{Friction term} + \overbrace{\left(\rho_L - \rho_G\right) g \sin\theta}^{\text{Weight term}}}{\underbrace{\left(\rho_L - \rho_G\right) g \cos\theta}_{\text{Hydrostatic pressure term}} - \underbrace{\rho_L v_L \frac{\left(u_T - u_{LS}\right) R_{LS}}{R_{LB}^2} \frac{dR_{LB}}{dh}}_{\text{Liquid inertial term}} - \underbrace{\rho_G v_G \frac{\left(u_T - u_{GS}\right)\left(1 - R_{LS}\right)}{\left(1 - R_{LB}\right)^2} \frac{dR_{LB}}{dh}}_{\text{Inercial gas term}}} \tag{3}$$

Equation (3) is the same as the one found by Taitel and Barnea (1990) and represents the slope of the tangent line to the shape of the elongated bubble. Thus, the equation is the ratio between friction terms plus the term weight and the hydrostatic pressure term plus inertial terms of the phases. But all these terms depend on the height of the liquid. Thus, it is not possible to solve this equation analytically and an algorithm is necessary to solve it numerically. This algorithm is presented in the next section.

3. NUMERICAL IMPLEMENTATION

This section presents the numerical implementation used to solve Eq. (3) and to compute the profile of the elongated bubble. The program was implemented in the commercial software Matlab. Figure 3 represents the flowchart of the algorithm developed to solve Eq. (3).

3.1 Input data

In order to solve the model and to determine the shape of the elongated bubble some input data are necessary. They are the diameter, slope and roughness of the pipe; the density, viscosity and superficial velocities of the gas and liquid phases and the surface tension between the phases are required as well. Additionally, it is necessary to know the length and the void fraction of the unit cell.

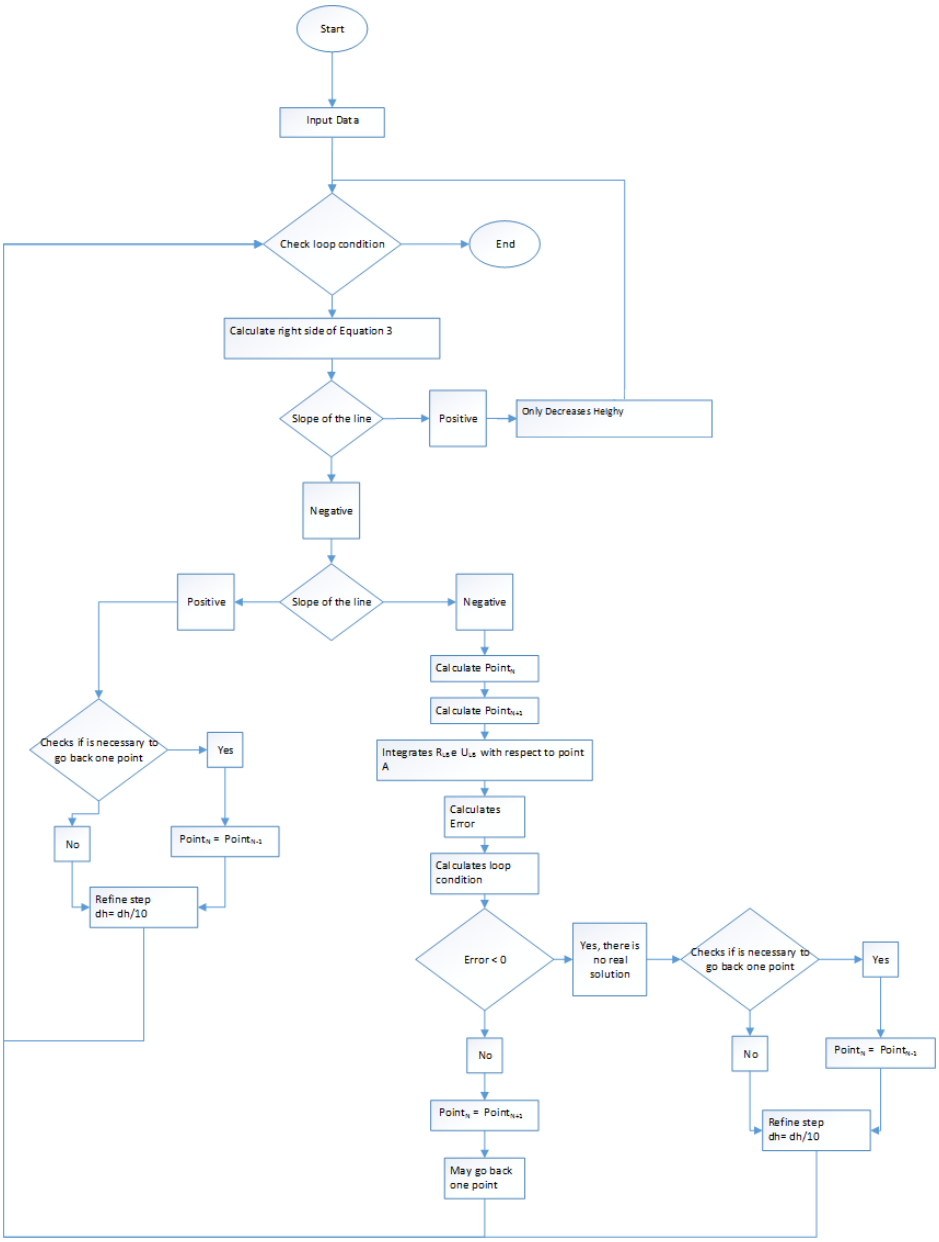

Figure 3. Program's flowchart.

3.2 Loop Structure

A variable dh scheme was used to minimize the execution time of the program. Defining β as the ratio between the length of the elongated bubble and that of the unit cell:

$$\beta = \frac{\overline{l}_B}{l_U} = \frac{\overline{l}_B}{l_B + l_S} \tag{4}$$

The convergence criterion is met when the mass balance of the unit cell is satisfied. Isolating β in the mass balance of the unit cell comes:

$$\beta_M = 1 - \frac{j_L - \overline{u}_{LB}\overline{R}_{LB}}{u_T R_{LS}\left(1 - \dfrac{\overline{R}_{LB}}{R_{LS}}\right)} \tag{5}$$

Thus, we can define an error between the two ways of calculating β. When this error reaches zero the bubble satisfies the convergence criterion and the program stops calculating the bubble profile.

The length of the unit cell is constant, but the length of the bubble increases as the number of completed loops increase, thus increasing β as well. And since $\bar{u}_{LB}$ and $\bar{R}_{LB}$ are decreasing, β_M tends to decrease.

The variable dh scheme is built so that a smaller dh can be used and whenever the error is negative the program goes back to the previous step, refines dh and calculates the next one. Thus, more points in the neighborhood of the bubble rear must be calculated by the program so that procedure converges. And since near the bubble tail a small increment of dh causes a large variation in x, convergence becomes rather tricky. Thence, refining the step in the bubble tail is helpful in finding the bubble length optimally.

In Figure 4 illustrates this scheme. As the calculation procedure approaches the tail of the bubble the points in the chart get farther from each other as long as *x*/D decreases (as the height is constant the variation in the *y*-axis will always remain almost constant). But at the neighborhood of the tail (towards the left side of the chart) they get very close again. This happens because the model has not found a solution, after that refine the step and then the profile was presented.

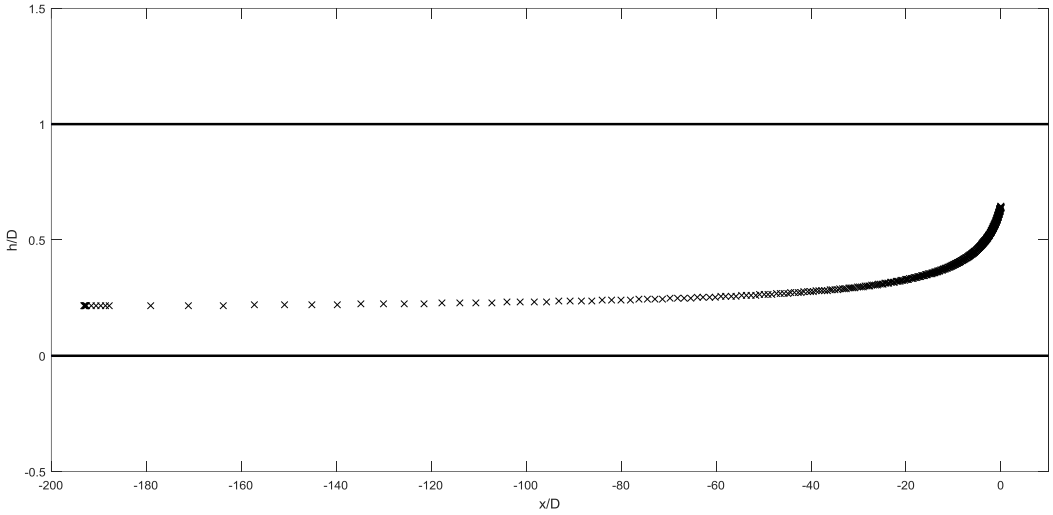

Figure 4 - Profile of elongated bubble calculated for surface velocities of air and water of 3 m/s and 0.5 m/s respectively.

3.3 Results of the Program.

Eventually the program yields the elongated bubble length l_B, the average velocity of the liquid film U_{LB}, the fraction of liquid and gas in the elongate bubble region R_{LB} and R_{GB} respectively and the profile of the elongate bubble.

4. RESULTS

The model was validated with experimental data from Rodrigues (2015). The data is for a horizontal flow of air and water. The pipe is 9-m long and has and ID of 0.0258 m. Table 1 shows the superficial velocities of each point, ranging from 0.25 to 3.03 m/s for water and 0.50-2.00 m/s for air. For all these points, numerical results were obtained and were then compared with the experimental data.

Table 1 – Points 1 to 15 of horizontal flow provided by de Rodrigues (2015).

Points	**1**	**2**	**3**	**4**	**5**	**6**	**7**	**8**	**9**	**10**	**11**	**12**	**13**	**14**	**15**
j_G(m/s)	3.00	1.75	2.26	2.76	1.51	2.00	2.51	3.01	0.75	1.25	1.75	2.26	2.76	0.50	1.00
j_L(m/s)	0.50	0.75	0.75	0.75	1.00	1.00	1.00	1.00	1.25	1.25	1.25	1.25	1.25	1.50	1.50

Table 2 – Continuation of Table 1 (points 16-29).

Points	**16**	**17**	**18**	**19**	**20**	**21**	**22**	**23**	**24**	**25**	**26**	**27**	**28**	**29**
j_G(m/s)	1.50	2.01	2.50	3.03	0.25	0.75	1.26	1.75	2.25	2.76	0.50	1.00	1.50	2.00

j_L(m/s)	1.50	1.50	1.50	1.50	1.75	1.75	1.75	1.75	1.75	1.75	2.00	2.00	2.00	2.00

The validation of the results with data measured experimentally by the electrode mesh sensor, originated three graphs comparing the results of the model with the said data. In Figure 5 the numerical and experimental values from R_{GB} are compared. The results can be regarded as good, since the biggest errors were slightly larger than 15%. Figure 6 presents the comparison between the bubble lengths measured experimentally and calculated by the model. Again, the model obtained good results, as most of the results were close to those measured experimentally with maximum errors of 10%. Figure 7 shows the comparison between the results for the slug length. In this case the errors approach 25%, but in several cases the errors are quite small. One of the causes of the slug length error being greater than the bubble length error comes from the fact that the slug distribution is best characterized by a log-normal curve (Vicencio, 2013 and Brill, 1981).

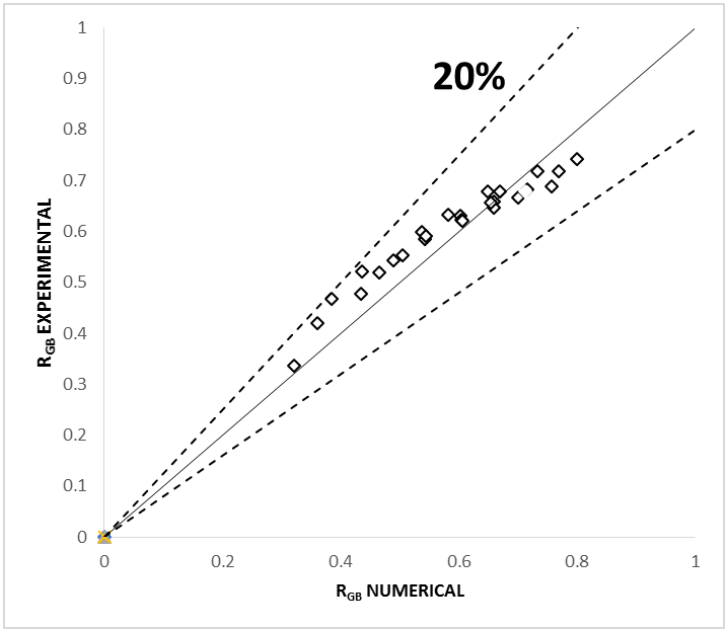

Figure 5 Comparison between the void fractions (numerical and experimental).

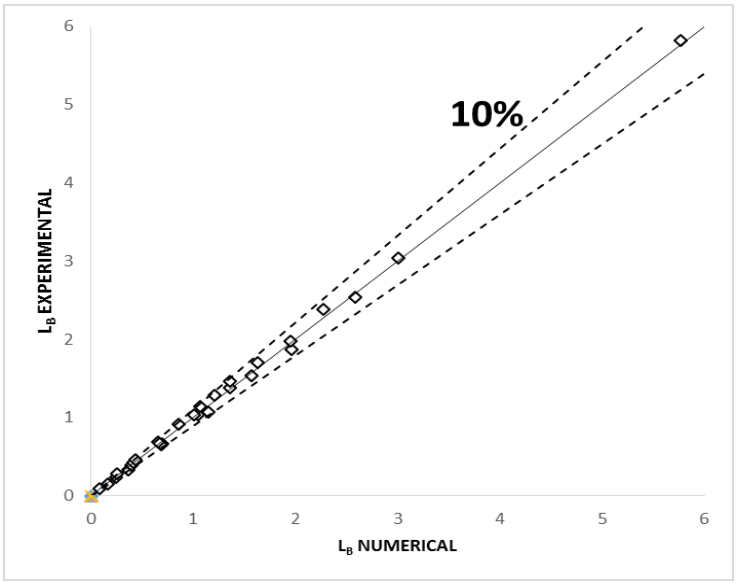

Figure 6. Comparison between the elongated bubble lengths (numerical and experimental).

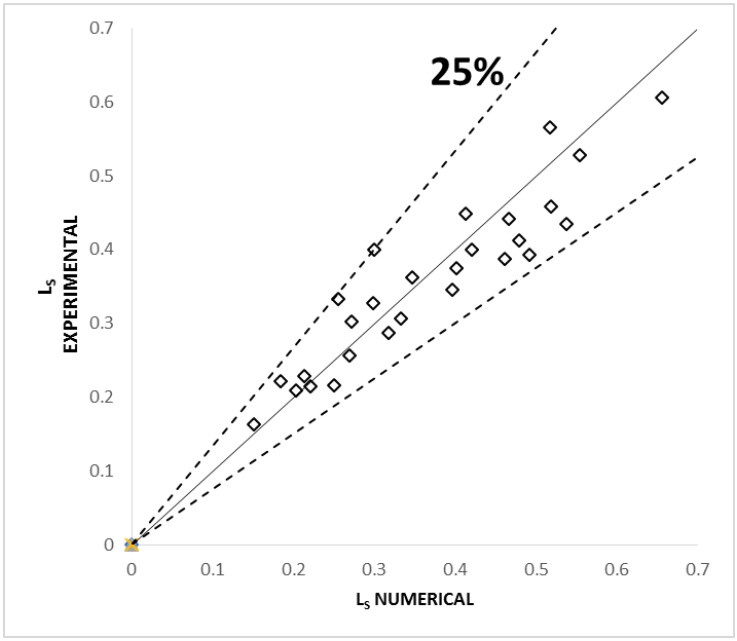

Figure 7. Comparison between the slug lengths (numerical and experimental).

Three bubble profiles, all with a mixture velocity of 3.5 m/s, were calculated so as to investigate the influence of the velocity of the mixture on the bubble profile. Those profiles are shown in Figure 8 for points 1, 4 and 7. It can be seen that the profile depends on the speed of the mixture, an outcome that is in agreement with the results obtained by Grenier *et al*. (1997), Woods *et al*.(1996) and Hanyang and Liejin (2016).

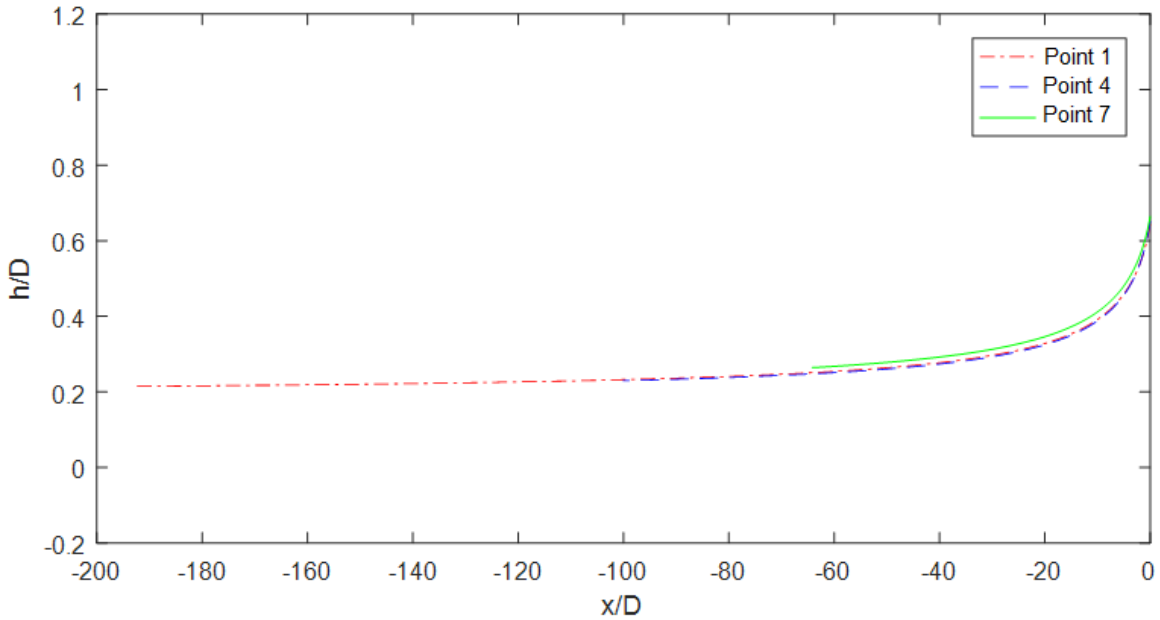

Figure 8. Profile of the elongated bubble at three points with a mixture velocity equal to 3.5 m/s. Point 1 has gas and liquid superficial velocities equal to 3 m/s and 0.5 m/s respectively. Point 4 has gas and liquid superficial velocities equal to 2.76 m/s and 0.75 m/s respectively. Point 7 has gas and liquid superficial velocities equal to 2.5 m/s and 1.0 m/s respectively.

5. CONCLUSIONS

A theoretical and experimental study on the profile of elongated bubbles in horizontal flows was carried out. The experiments showed that the bubble profile varies with the same velocity of the mixture. A theoretical model for calculating the bubble profile was presented. An optimized scheme for calculating the bubble profile was presented and

gauged. The validation of the model using experimental data showed good results and proved that the model can calculate the length of the elongated bubble, the void fraction and the slug length within a fairly good accuracy.

6. REFERENCES

Bendiksen, K. H. An experimental investigation of the motion of long bubbles in inclined tubes. International Journal of Multiphase Flow, Vol. 10, p. 467-483, 1984.

Brill, James P., et al. "Analysis of two-phase tests in large-diameter flow lines in Prudhoe Bay field." *Society of Petroleum Engineers Journal* 21.03 (1981): 363-378.

Dukler, Abraham E., and Martin G. Hubbard. "A model for gas-liquid slug flow in horizontal and near horizontal tubes." *Industrial & Engineering Chemistry Fundamentals* 14.4 (1975): 337-347.

Falcone, Gioia, Geoffrey Hewitt, and Claudio Alimonti. *Multiphase flow metering: principles and applications*. Vol. 54. Elsevier, 2009.

Grenier, P., J. Fabre, and J. R. Fagundes Netto. "Slug flow in pipelines: recent advances and future developments." BHR Group Conference Series Publication. Vol. 24. Mechanical Engeneering Publications Limited, 1997.

Hanyang, Gu, and Guo Liejin. "Modeling of bubble shape in horizontal and inclined tubes." *Progress in Nuclear Energy* 89 (2016): 88-101.

Netto, JR Fagundes, J. Fabre, and L. Peresson. "Shape of long bubbles in horizontal slug flow." *International Journal of Multiphase Flow* 25.6 (1999): 1129-1160.

Rodrigues, Romulo Luis de Paiva. *Caracterização experimental do escoamento bifásico de gás-líquido descendente em golfadas em tubulações levemente inclinadas*. MS thesis. Universidade Tecnológica Federal do Paraná, 2015.

Taitel, Yehuda, and Dvora Barnea. "Two-phase slug flow." *Advances in heat transfer* 20 (1990): 83-132.

Vicencio, Fernando Enrique Castillo. *Caracterização experimental do escoamento intermitente líquido-gás em tubulações horizontais*. MS thesis. Universidade Tecnológica Federal do Paraná, 2013.

Wallis, Graham B. "One-dimensional two-phase flow." (1969).

Woods, B. D., and T. J. Hanratty. "Relation of slug stability to shedding rate." *International journal of multiphase flow* 22.5 (1996): 809-828.

7. RESPONSIBILITY NOTICE

The authors are the only responsible for the printed material included in this paper.